

RESEARCH LETTER

Gut ACE2 Expression, Tryptophan Deficiency, and Inflammatory Responses: The Potential Connection That Should Not Be Ignored During SARS-CoV-2 Infection

An “atypical” physiological function of angiotensin-converting enzyme 2 (ACE2) during COVID-19 is rarely mentioned. In the intestine, where ACE2 is highly expressed,¹ it acts as a regulator of the homeostasis of dietary amino acids, particularly tryptophan (Trp). Trp catabolism through the kynurenine (Kyn) pathway plays an important role in regulating the balance between effector and regulatory immune responses; Trp catabolism is increased in inflammatory settings to attenuate excessive systemic immune activation and thus exerts protective effects against many diseases.^{2,3}

Given that interaction with SARS-CoV-2 decreases the cell surface expression of ACE2 by endocytosis and ADAM17 cleavage,⁴ we performed a preliminary study and proposed a hypothesis that SARS-CoV-2 infection downregulates ACE2 expression in intestinal epithelial cells, reduces Trp absorption, and thus disrupts the local and systemic inflammatory responses. This hypothesis provides a possible reason for the digestive symptoms and hyperinflammatory phenotypes of patients with COVID-19.

We treated mice with recombinant SARS-CoV-2 spike protein (receptor binding domain [RBD]) to mimic SARS-CoV-2 infection and further challenged the mice with lipopolysaccharide (LPS) to induce a hyperinflammatory status. LPS stimulation reduced the serum Trp levels of the mice in both the control and RBD groups (Figure 1A), and this effect was accompanied by elevated Kyn levels

and Kyn/Trp ratios (Figure 1B, Supplementary Figure 1A); these results suggested the increased catabolism of Trp to Kyn and higher levels of inflammation. Although the Kyn/Trp ratios in the RBD group were similar to those in the control group (Supplementary Figure 1A), the RBD-treated mice showed lower serum Trp and Kyn levels than the untreated mice regardless of LPS stimulation (Figure 1A and B).

To further verify our results, we analyzed the metabolomic data from a published article.⁵ The serum levels of Trp and Kyn in COVID-19 patients were significantly lower than those in healthy persons and non-COVID-19 pneumonia patients; however, the Kyn/Trp ratios were comparable (Figure 1C and D, Supplementary Figure 1B). The levels of other important metabolites of Trp, such as quinolinate and serotonin, were also decreased in COVID-19 patients (Supplementary Figure 1C and D).

Immunofluorescence staining showed that ACE2 expression on the surface of intestinal epithelial cells was significantly decreased in RBD-treated mice (Figure 1E). Similarly, ACE2 expression on the surface of MOD-K and HNM460 cells, 2 kinds of intestinal epithelial cells from mice and humans, was also notably decreased after *in vitro* treatment with RBD and S1 protein (another SARS-CoV-2 spike protein) (Figure 1F and G). The serum Trp levels of ACE2-deficient mice (ACE2^{KO}) were lower than those of wild-type mice, and RBD administration did not reduce the serum Trp levels in the ACE2^{KO} mice treated with or without LPS (Figure 1H), suggesting a central role of ACE2 in the Trp deficiency induced by SARS-CoV-2 infection.

Furthermore, no significant difference was observed in the serum levels of inflammatory cytokines between the control animals and RBD-treated mice (Supplementary Figure 2A), indicating that RBD alone could not induce a systemic inflammatory response. However, RBD administration significantly

enhanced LPS-induced hyperinflammation in mice, as evidenced by increased levels of proinflammatory cytokines (IFN γ , IFN α , IFN β , TNF α , IL1 β , and IL6), decreased levels of anti-inflammatory cytokines (IL10) (Figure 1I, Supplementary Figure 2B-E), and aggravated local infiltration of inflammatory cells and injury to the lung and liver (Supplementary Figure 3). The effect of RBD was negated or even reversed by L-Trp supplementation or ACE2 depletion (Figure 1I and J, Supplementary Figure 2B-E). When challenged with a sublethal dose of LPS (25 mg/kg), the RBD-treated group showed poorer survival than the control group (Figure 1K). Notably, resupplying mice with L-Trp greatly improved survival in the control and RBD-treated groups and abolished the difference between these groups (Figure 1K).

Here, we found that Trp deficiency is a prominent characteristic and an important driving factor of the pathobiology of COVID-19. Nearly 50.5% of COVID-19 patients report digestive symptoms; Trp deficiency has been proven to enhance susceptibility to Dextran sulphate sodium, DSS-induced colitis.² These findings allow us to infer that digestive symptoms of COVID-19 patients may be partly attributed to disrupted Trp homeostasis.

More importantly, by activating the aryl hydrocarbon receptor pathway and allowing the generation of regulatory T cells, Kyn plays a critical role in regulating disease tolerance and immune homeostasis.⁶ Our results suggested that alterations in the Kyn pathway impair the negative self-regulatory capacity of the immune system and thus promote the occurrence of hyperinflammation and cytokine storm syndrome, which makes COVID-19 more lethal.

Moreover, the Kyn pathway provides raw materials for the synthesis of nicotinamide adenine dinucleotide (NAD), which is important for regulating oxidative stress and DNA

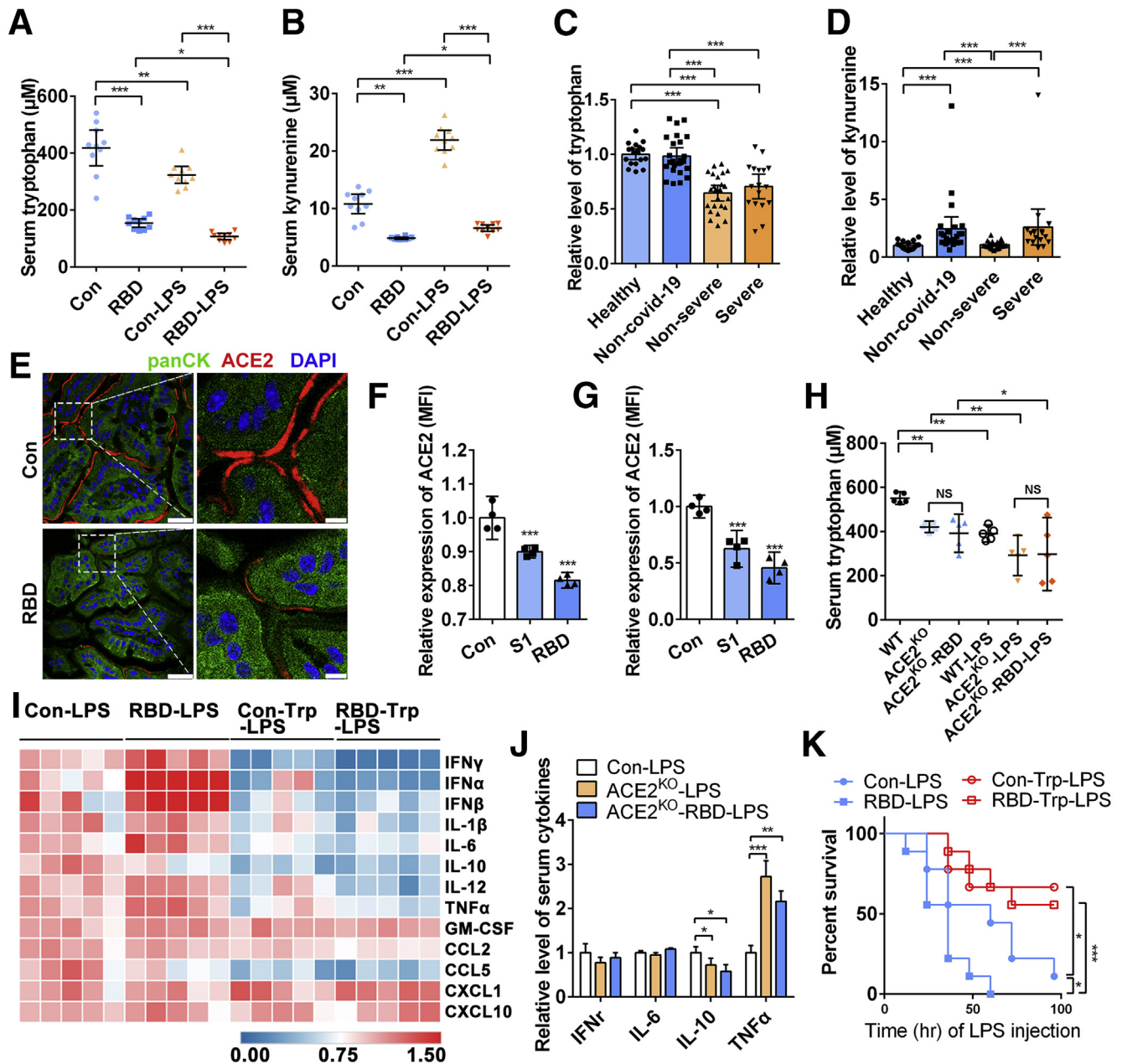


Figure 1. Serum levels of Trp (A) and Kyn (B) in mice ($n = 10$). Relative serum levels of Trp (C) and Kyn (D) in healthy control subjects, non-COVID-19 pneumonia patients, nonsevere COVID-19 patients, and severe COVID-19 patients. (E) Representative immunofluorescence images of ACE2 (red) and panCK (green) counterstained with DAPI (blue) in the intestinal tissue of mice. Expression of ACE2 in MOD-K (F) and HNM460 cells (G). (H) Serum levels of Trp in wild-type (WT) and ACE2 knockout (ACE2^{KO}) mice ($n = 5$). (I) Serum levels of cytokines in LPS-challenged mice treated with or without RBD and L-Trp ($n = 5$). (J) Serum levels of cytokines in WT and ACE2^{KO} mice treated with or without LPS, RBD, or L-Trp ($n = 5$). (K) Survival of mice challenged with lethal levels of LPS and treated with or without RBD and L-Trp ($n = 9$). * $p < 0.05$, ** $p < 0.01$, *** $p < 0.001$.

damage repair. Recent studies revealed that SARS-CoV-2 infection might decrease repletion of the NAD metabolome from Trp,⁷ and supplementation with NAD could effectively reverse cytokine storms and organ damage.⁸

Therefore, NAD supplementation may be a potential explanation for the therapeutic effect of L-Trp on SARS-CoV-2-related hyperinflammation.

Overall, as shown in Figure 2, attention should be given to the effect

of ACE2-mediated Trp deficiency on the course of COVID-19. Further research is needed to pave the way for the development of new strategies to modulate COVID-19 by targeting Trp metabolism.

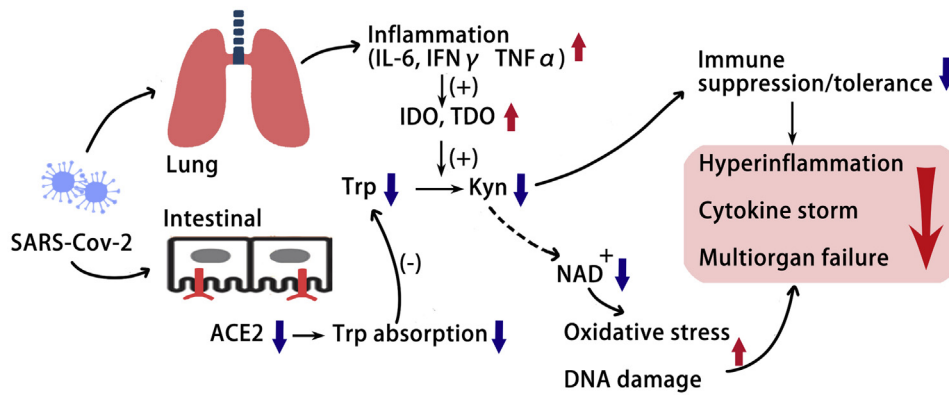


Figure 2. Schematic diagram of the role of SARS-CoV-2-induced Trp deficiency in the pathobiology of COVID-19.

W.-H. QIN^{1,2,a}

C.-L. LIU^{1,3,a}

Y.-H. JIANG^{1,3}

B. HU²

H.-Y. WANG^{1,3,4}

J. FU^{1,3,5}

¹International Cooperation Laboratory on Signal Transduction, Eastern Hepatobiliary Surgery Hospital, Second Military Medical University, Shanghai, China

²Department of Gastroenterology and Endoscopy, Eastern Hepatobiliary Surgery Hospital, Second Military Medical University, Shanghai, China

³National Center for Liver Cancer, Shanghai, China

⁴Ministry of Education Key Laboratory on Signaling Regulation and Targeting Therapy of Liver Cancer, Shanghai Key Laboratory of Hepato-biliary Tumor Biology, Shanghai, China; and ⁵Mengchao Hepatobiliary Hospital, Fujian Medical University, Fuzhou, China

Corresponding author: Jing Fu, MD, PhD, International Cooperation Laboratory on Signal Transduction, Eastern Hepatobiliary Surgery Hospital, Second Military Medical University, 225

Changhai Road, Shanghai 200438, China. e-mail: fujing-724@163.com. fax: (86) 21 6556 6851; and Hongyang Wang, PhD, International Cooperation Laboratory on Signal Transduction, Eastern Hepatobiliary Surgery Hospital, Second Military Medical University, 225 Changhai Road, Shanghai 200438, China. e-mail: hywangk@vip.sina.com; fax: (86) 21 6556 6851.


References

1. Hamming I, et al. *J Pathol* 2004; 203:631–637.
2. Hashimoto T, et al. *Nature* 2012; 487:477–481.
3. Neurath MF. *Gut* 2020; 69:1335–1342.
4. Wang K, et al. *Circulation* 2020.
5. Shen B, et al. *Cell* 2020;182:59–72.
6. Bessede A, et al. *Nature* 2014; 511:184–190.

7. Heer C, et al. *J Biol Chem* 2020; 295:17986–17996.

8. Hong G, et al. *Free Radic Biol Med* 2018;123:125–137.

^aAuthors contributed equally to this work.

 Most current article

© 2021 The Authors. Published by Elsevier Inc. on behalf of the AGA Institute. This is an open access article under the CC BY-NC-ND license (<http://creativecommons.org/licenses/by-nc-nd/4.0/>). 2352-345X

<https://doi.org/10.1016/j.jcmgh.2021.06.014>

Received March 30, 2021. Accepted June 21, 2021.

Conflicts of interest

The authors disclose no conflicts.

Funding

This work was funded by the National Natural Science Foundation of China (82003005, 81872231, 82073411), Shanghai Committee of Science and Technology (20YF1459100).

Supplementary Methods

Animal Models

The C57BL/6J mice and ACE2^{KO} mice were obtained from Shanghai Model Organisms. All mice in experiments were sex- and age-matched. All mice were bred at the animal facility of the National Center for Liver Cancer, according to the National Center for Liver Cancer Animal Care and Use Committee guidelines. All experiments were according to the National Institutes of Health Guide for the Care and Use of Laboratory Animals, with the approval of the Scientific Investigation Board of the Second Military Medical University, Shanghai.

The SARS-CoV-2 Spike Protein Imitated Virus Infection in Mice

SARS-CoV-2 Spike RBD-His Recombinant Protein (40592-V08H) and SARS-CoV-2 Spike S1-His Recombinant Protein (40591-V08H) were obtained from Sino Biological, Shanghai. Eight-week-old C57BL/6J and ACE2^{KO} mice were intraperitoneally injected with RBD (dissolved with normal saline to 0.075 $\mu\text{g}/\mu\text{L}$, 0.15 mg/kg body weight per mouse, daily in 3 days) to imitate infection of SARS-CoV-2. The LPS (L2630, Sigma-Aldrich, St. Louis, MO) was intraperitoneally injected to induce inflammation.

Secondary Analysis of Published Data

Data of published article were obtained from ProteomeXchange Consortium (<https://www.iprox.org/>) with project ID: IPX0002106000 and IPX0002171000. A total of 83 samples had matched proteomic and metabolomic data. The samples are divided into healthy, non-COVID-19 pneumonia, nonsevere COVID-19, and severe COVID-19 groups according to the index number. Then the serum relative levels of Trp, Kyn, serotonin, and quinolinate were analyzed. Proteins whose expression level was significantly correlated with the levels of Trp or Kyn were selected using Spearman correlation analysis, with a criteria that $r \geq 0.3$ or ≤ -0.3 , and $P \leq .05$.

Cell Culture and Administration

MODE-K (F) and NCM460 (Zhong-qiaoxin Zhou, Shanghai, China) cells were cultured in RPMI 1640 (Gibco, Thermo Fisher Scientific, Waltham, MA) containing 10% fetal bovine serum, 100 units of penicillin, and 100 mg/mL streptomycin. Cells were digested by 0.5% trypsin for 2 minutes to passage. To imitate virus infection, 500x S1 (40591-V08H SinoBiological, Shanghai, China) and RBD (40592-V08H, SinoBiological, Shanghai, China) protein were used to stimulate cells for 6 hours, respectively.

Flow Cytometry

For flow cytometric analyses of ACE2 expression, cells were placed on ice in 100 μL flow cytometry staining buffer (1% bovine serum albumin plus 0.1% sodium azide in phosphate-buffered saline). Fc γ receptors were blocked with CD16/32 blocking antibody for 10 minutes at 4°C before staining. For surface antigen staining, cells were stained with antibodies (ab15348, Abcam, Cambridge, UK) for 30 minutes at 4°C. Live cells were gated according to their forward scatter (FSC-H) and side scatter (SSC-H); single cells were gated according to their FSC-W and SSC-H.

Hematologic Analysis, Serum Metabolites Detection, and Multicytokines Flow Assay

Whole blood was collected from orbit, and then centrifuged at 4°C, 1500 rpm for 15 minutes to collect serum.

The serum levels of Trp and Kyn were determined by Nexera UHPLC LC-30AT and SCIEX 5600+ Mass Spectrometer. Briefly, 30 μL serum is added with 60 μL cold acetonitrile, ultrasonic in ice and bath for 30 minutes, after centrifuge at 4°C, 12,000 rpm for 10 minutes, and supernatant is taken for detection.

For multicytokine flow assay, the serum was centrifuged for 3000 rpm, 10 minutes at 4°C, and supernatant collected. The 13 mouse cytokines (IFN- γ , CXCL1, TNF- α , CCL2, IL-12, CCL5, IL-1 β , CXCL10, GM-CSF, IL-10, IFN- β , IFN- α , and IL-6) in serum were

detected and analyzed by the LEG-ENDplex MU Anti-Virus Response Panel (Biolegend, San Diego, CA) under kit direction.

Hematoxylin-Eosin Staining and Immunofluorescence Staining

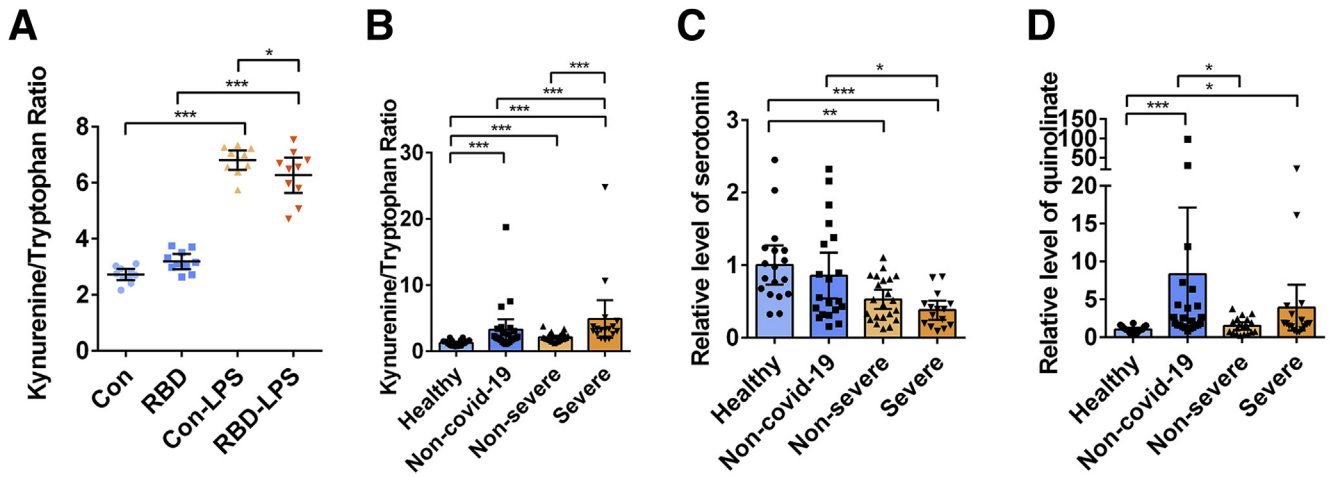
Tissues were dipped in 4% paraformaldehyde and embedded in paraffin after dehydration, and cut into 8- μm -thick slices. The slices were deparaffinized and stained with hematoxylin and eosin and examined.

The lung injury scores were determined by the following methods. Three fields were randomly chosen from each section (15 fields, each group). Four pathologic features of alveolar congestion, immune cell infiltration, alveolar thickness, and hyaline membrane formation were evaluated in each field, and scored in the range of 0–4.

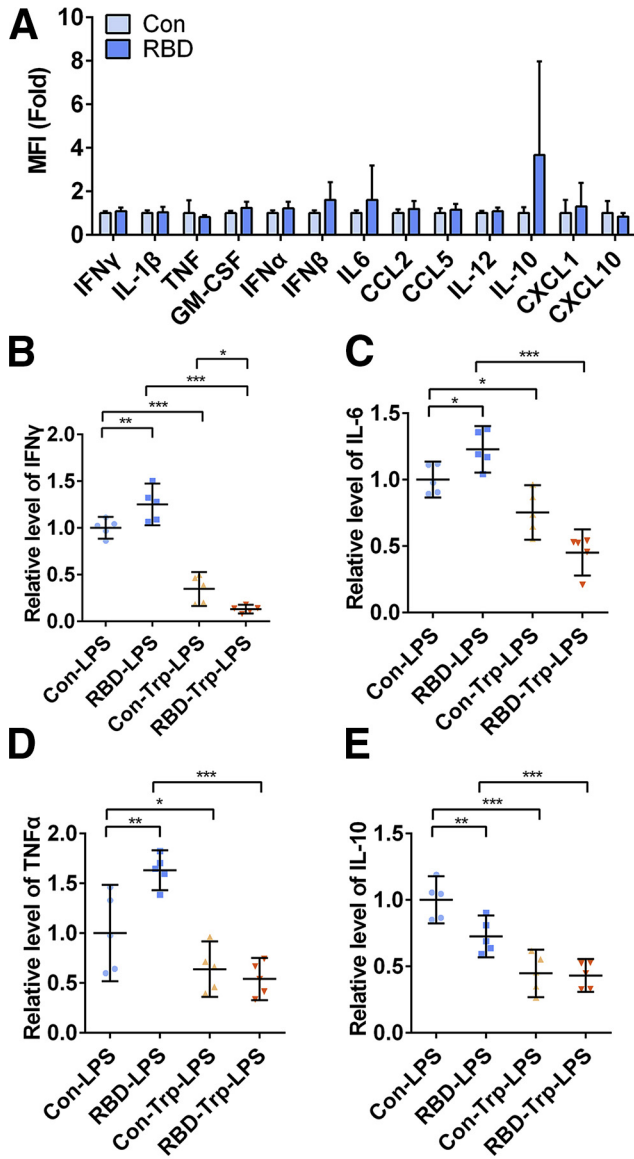
For immunofluorescence staining, briefly, antigen was retrieved by sodium citrate buffer (pH 6.0) and boiled in the oven for 3 minutes. Then, blocked at 37°C for 30 minutes with 1% bovine serum albumin and following incubated with ACE2 and pan-Cytokeratin antibody mixture (ab15348 and ab215838, diluted at 1:50, Abcam at 4°C overnight. A goat antirabbit-IgG AF488 and a goat antimouse-IgG AF555 was used as secondary at RT for 1 hour. DAPI was diluted at 1:1000 to dyeing nucleus for 10 minutes.

Statistical Analysis

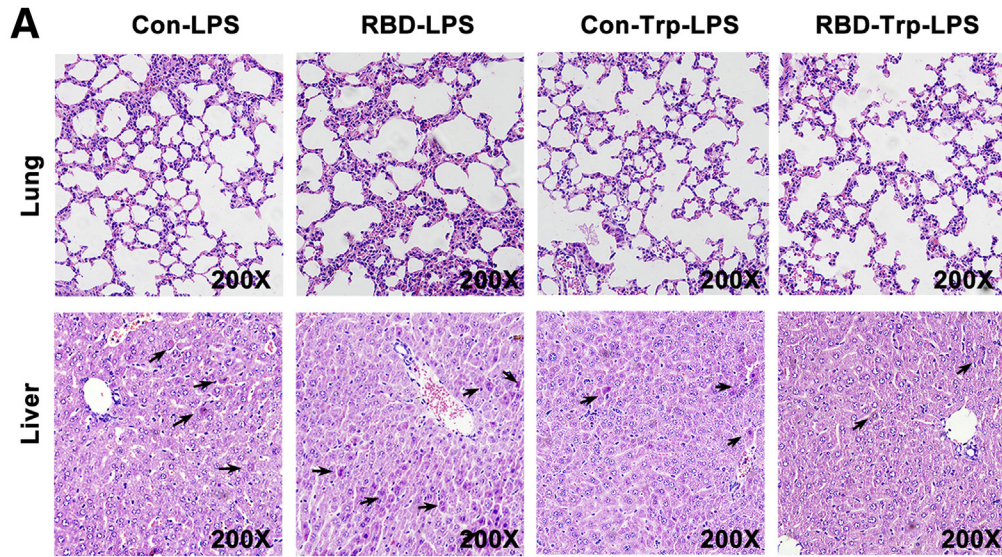
All statistical analyses were performed using the statistical software (SPSS version 21). Experimental data were depicted as mean \pm standard error of mean. A 2-tailed Student *t* test was used when there were only 2 groups for analysis, analysis of variant test was used for analysis of more than 2 groups throughout data, and LSD-*t* test was used for multiple comparison. Assessment of differences in nonnormal distribution data was performed using nonparametric Mann-Whitney *U* tests. A *P* value of $\leq .05$ was considered statistically significant. In all figures, **P* $\leq .05$, ***P* $\leq .01$, and ****P* $\leq .001$.



Supplementary Figure 1. Serum levels of Trp and its metabolites in mice and human. (A) The ratio of serum Kyn/Trp in mice treated with or without RBD and LPS. (n = 10). The ratio of serum Kyn/Trp (B), serum levels of serotonin (C), and quinolinate (D) in healthy, non-COVID-19 pneumonia patients, nonsevere COVID-19 patients, and severe COVID-19 patients. The data are representative of 3 (A) independent experiments, and analyzed by 1-way analysis of variance (A), Mann-Whitney test (B-D). The data indicate the mean \pm 95% confidence intervals. * $P < .05$, ** $P < .01$, and *** $P < .001$. NS, not significant.



Supplementary Figure 2. Serum levels of cytokines in mice. (A) Serum levels of cytokines in mice treated with or without RBD. (n = 5). Serum levels of IFN γ (B), IL6 (C), TNF α (D), and IL10 (E) in LPS-challenged mice treated with or without RBD and L-Trp (n = 5). The data are representative of 2 independent experiments, and analyzed by unpaired Students *t* test (A) and 1-way analysis of variant analysis (B-E). The data indicate the mean \pm 95% confidence intervals. **P* < .05, ***P* < .01, and ****P* < .001. NS, not significant.



Supplementary Figure 3. Histopathological analyses of lung and liver injury. Representative images of the hematoxylin-eosin staining of lung and liver paraffin sections; necrotic hepatocytes indicated by *black arrow* (A). Lung injury score (B) and necrotic hepatocyte counts (C) were used to assess target organ damage caused by hyperinflammation (n = 10). The data are representative of 2 (B and C) independent experiments, and analyzed by 1-way analysis of variant analysis (B and C). The data indicate the mean ± 95% confidence intervals. **P* < .05, ***P* < .01, and ****P* < .001. NS, not significant.

